

Y. Liang, P. Lomas, I. Nunes, M. Gryaznevich, M.N.A. Beurskens, S. Brezinsek,
J. W. Coenen, P. Denner, Th. Eich, L. Frassinetti, S. Gerasimov, D. Harting,
S. Jachmich, A. Meigs, J. Pearson, M. Rack, S. Saarelma, B. Sieglin,
Y. Yang, L. Zeng and JET EFDA contributors

Mitigation of Type-I ELMs with $n = 2$ Fields on JET with ITER-like Wall

“This document is intended for publication in the open literature. It is made available on the understanding that it may not be further circulated and extracts or references may not be published prior to publication of the original when applicable, or without the consent of the Publications Officer, EFDA, Culham Science Centre, Abingdon, Oxon, OX14 3DB, UK.”

“Enquiries about Copyright and reproduction should be addressed to the Publications Officer, EFDA, Culham Science Centre, Abingdon, Oxon, OX14 3DB, UK.”

The contents of this preprint and all other JET EFDA Preprints and Conference Papers are available to view online free at www.iop.org/Jet. This site has full search facilities and e-mail alert options. The diagrams contained within the PDFs on this site are hyperlinked from the year 1996 onwards.

Mitigation of Type-I ELMs with $n = 2$ Fields on JET with ITER-like Wall

Y. Liang¹, P. Lomas², I. Nunes², M. Gryaznevich², M.N.A. Beurskens², S. Brezinsek¹,
J.W. Coenen¹, P. Denner¹, Th. Eich³, L. Frassinetti⁴, S. Gerasimov², D. Harting¹,
S. Jachmich⁵, A. Meigs², J. Pearson¹, M. Rack¹, S. Saarelma², B. Sieglin³,
Y. Yang¹, L. Zeng¹ and JET EFDA contributors*

JET-EFDA, Culham Science Centre, OX14 3DB, Abingdon, UK

¹*Forschungszentrum Jülich GmbH, Association EURATOM-FZ Jülich, Institut für Energie- und Klimaforschung - Plasmaphysik, Trilateral Euregio Cluster, D-52425 Jülich, Germany*

²*EURATOM-CCFE Fusion Association, Culham Science Centre, OX14 3DB, Abingdon, OXON, UK*

³*Max-Planck-Institut für Plasmaphysik, EURATOM-Assoziation, D-85748 Garching, Germany*

⁴*Association EURATOM-VR, Fusion Plasma Physics, EES, KTH, SE-10044 Stockholm, Sweden*

⁵*Association EURATOM-Belgian State, Koninklijke Militaire School - Ecole Royale Militaire, B-1000 Brussels Belgium*

** See annex of F. Romanelli et al, "Overview of JET Results", (24th IAEA Fusion Energy Conference, San Diego, USA (2012)).*

ABSTRACT

Mitigation of type-I Edge Localized Modes (ELMs) has been observed with the application of an $n = 2$ field in H-mode plasmas on the JET tokamak with the ITER-like wall. In high collisionality ($\nu_e^* \sim 2.0$) H-mode plasmas, large type-I ELMs with a frequency of ~ 45 Hz were replaced by high frequency (a few hundred Hz) small ELMs during the application of the $n = 2$ field. No density pump-out was observed. The influence of the $n = 2$ field on the core and pedestal electron pressure profiles is within the error bars and can be neglected. Splitting of the outer strike point has been observed during the strong mitigation of the type-I ELMs. The maximal surface temperature (T_{\max}) on the outer divertor plate was saturated and has only small variations of a few degrees due to the small mitigated ELMs. In low collisionality ($\nu_e^* \sim 0.8$) H-mode plasmas, the ELM frequency increased by a factor of four (from ~ 20 to ~ 80 Hz). Clear density pump-out was observed during the application of the $n = 2$ field. The effect of ELM mitigation with the $n = 2$ field was seen to saturate so that the ELM frequency did not increase further above a certain level of $n = 2$ magnetic perturbations. Multiple splitting of the outer strike point during the ELM crash has been seen, resulting in mitigation of the maximal ELM peak heat fluxes on the divertor region.

1. INTRODUCTION

A reliable method for Edge Localized Mode (ELM) control is needed for ITER to handle the peak heat loads onto the Plasma Facing Components (PFCs) [1, 2]. Recently obtained results from several tokamaks (DIII-D [3], JET [4], MAST [5], NSTX [6], AUG [7] and KSTAR [8]) have shown that magnetic field perturbations can either completely suppress ELMs, or affect the frequency and size of the type-I ELMs in a controllable way while preserving good global energy confinement. The coil systems in these devices include different designs, e.g. in-vessel off-midplane coils and external midplane coils. Each design provides different poloidal, m , and toroidal, n , mode number spectra as well as different radial profiles. To date, suppression of the type-I ELMs has only been achieved by using in-vessel off-midplane coils in DIII-D ($n = 3$), AUG ($n = 2$) and KSTAR ($n = 1$). On JET, the type-I ELM frequency in low collisionality ($\nu_e^* \sim 0.1$) Hmode plasmas has been increased by a factor of up to 5 when applying static $n = 1$ or 2 fields produced by four external midplane error field correction coils (EFCCs) [9,10,11,12]. This raises an open question: What is the limitation for ELM control/suppression with external midplane coils?

To date, most of ELM mitigation/suppression experiments were performed on the devices with CFC-based PFCs. However, for the initial operation phase of ITER the divertor will be covered by carbon-fibre composites and tungsten, while a carbon-free tungsten divertor is foreseen for the operation phase with activation. The main chamber blanket modules in ITER are protected by shaped (limiter-like) beryllium panels. Therefore, it is urgent and important to prove the applicability of the ELM control/suppression with an external magnetic perturbation in the plasmas with ITER-like PFCs and systematic comparison with the previous results with CFC-based PFCs.

Recently, the ITER-like wall (ILW) has been installed on JET to replace the previous CFC-based

PFCs [13]. In addition, the JET EFCC power supply system has been enhanced with a coil current of up to 96kAt (twice as high as before [10]). A sufficient amount of the effective low n ($n = 1$, or 2) perturbation fields can be induced by the EFCCs for JET ELM control/suppression experiments over a wide range of plasma parameters. In this paper, mitigation of type-I ELMs with the $n = 2$ field in both low and high collisionality H-mode plasmas with the ILW is presented.

2. ELM CONTROL IN LOW COLLISIONALITY H-MODE PLASMAS WITH THE ILW

ELM control with an $n = 2$ field was investigated in low collisionality H-mode plasmas on JET with the ILW. In this experiment, the target type-I ELMy H-mode plasma ($I_p = 1.4\text{MA}$; $B_t = 1.85\text{T}$) was sustained by the Neutral Beam Injection (NBI) with a total input power of 9 MW as seen in Fig. 1. To avoid attachment of the plasma to the Be-wall, due to the 3D distortion of the plasma surface with applied $n = 2$ fields, the discharges were programmed in a slim low triangularity shape with a large gap between plasma and the wall. Strong gas puffing with a constant puffing rate of 3.0×10^{21} el/s was applied during NBI phase. The density Greenwald fraction number is ~ 0.7 , and the electron collisionality at the pedestal is ~ 0.8 .

The effect of the $n = 2$ field on the pedestal energy, W_{ped} , and the ELM energy loss, $\Delta W_{\text{ped}} = W_{\text{ped}}$, has been investigated for the mitigated ELMs with the $n = 2$ field as shown in Fig.2. The pedestal energy calculated from the measured electron profiles is $\sim 706\text{kJ}$ for the target type-I ELM plasma and $\sim 622\text{kJ}$ for the plasma with mitigated ELMs. Here, the electron temperature and density profiles were measured by the High Resolution Thomson Scattering (HRTS) on JET [14] [15]. Without the $n = 2$ field, the ELM energy loss is $\sim 67\text{kJ}$, which is $\sim 10\%$ of the pedestal energy. A clear crash in the pedestal pressure is mostly caused by a large drop in the pedestal density rather than a change in the pedestal temperature. With the $n = 2$ fields, the pedestal density dropped by $\sim 15\%$ (the so-called density pump-out effect) while the electron temperature increases by $\sim 15\%$, hence a small change in the pedestal pressure profile. Within the HRTS resolution, no clear drop was observed in either the pedestal density or temperature profiles, during the crash of the mitigated ELMs. The energy loss caused by the mitigated ELMs is $\sim 2\text{kJ}$ (0.5% of the pedestal energy), and is within the measurement error. The ELM energy loss scales inversely with the ELM frequency for the mitigated ELMs.

Previous experiments [9,10] on JET with CFC-based PFCs and $n = 2$ fields observe similar phenomena, i) increase in ELM frequency and drop in ELM size; ii) density pump-out; iii) strong non-resonant magnetic rotation braking. However, with the ILW and higher amplitude of magnetic perturbation, there are two major new observations: i) the effect of ELM mitigation with an $n = 2$ field was seen to saturate so that the ELM frequency did not increase further above a certain level of the EFCC coil current; ii) multiple splitting of the outer strike point during the ELM crash.

2.1 SATURATION EFFECT OF ELM MITIGATION WITH THE $n = 2$ FIELDS

Figure 1 shows two identical discharges with the only difference in the amplitude of I_{EFCC} , 38,4kAt

for the Pulse No: 82474 and 88 kAt for the Pulse No: 83469. The $n = 2$ fields were applied 1.5 seconds after the type-I H-mode was established. The EFCC coil current, I_{EFCC} , was ramped up slowly to the flat top with a ramp rate of 5kAt/s and was kept constant for a few seconds. A clear I_{EFCC} threshold for ELM mitigation was observed. The ELM frequency increases from $\sim 20\text{Hz}$ to $\sim 80\text{Hz}$ when I_{EFCC} is ramped up to 38.4kAt, and does not increase further even with an increase in IEFCC up to 88kAt. Here, it is named the saturation effect of ELM mitigation with $n = 2$ fields.

A set of saddle loops, which are fitted against the ex-vessel wall of each octant, have been used to measure both the amplitude and toroidal mode number (up to four) of the radial plasma fields on JET. They have been used regularly to detect locked modes. The plasma response to the applied $n = 2$ field, $|B_{n=2}^{\text{plasma}}|$, can be identified by subtracting the vacuum pick-up components from the measured $n = 2$ radial fields. In this experiment, the measured $n = 2$ radial fields are always smaller than the vacuum pick-up. This might be due to the rotation screening effect dominating the plasma response to the applied RMP field in a low beta plasma.

Figure 3 (left) shows the dependence of the plasma response on the normalized amplitude of the applied $n = 2$ magnetic perturbations, which is defined as the ratio of IEFCC to the toroidal field. Two regimes of the plasma responses to the applied $n = 2$ field, linear and non-linear regimes, have been identified. During the linear regime, $|B_{n=2}^{\text{plasma}}|$ linearly increases with increasing I_{EFCC} , while $|B_{n=2}^{\text{plasma}}|$ saturates for further increases in IEFCC during the non-linear regime. There is an I_{EFCC} threshold for the transition from the linear to the non-linear regime. The correlation between the plasma responses and the ELM mitigation with the $n = 2$ fields is shown in Fig.3 (right). In the linear regime, the ELM frequency (which increases from ~ 20 to $\sim 40\text{Hz}$) depends linearly on the amplitude of IEFCC. However, a sudden increase in the ELM frequency from $\sim 40\text{Hz}$ to $\sim 80\text{Hz}$ occurred at the transition from the linear to the non-linear plasma response. There is no clear change of the ELM frequency once the plasma response was saturated. This result indicates that the saturation effect of ELM mitigation with $n = 2$ fields might be due to the non-linear plasma response to the applied magnetic perturbations.

Enhancement of the density pump-out was observed after the transition of plasma response from the linear to non-linear regime as shown in Fig.4. The drop in density, n_e , saturates at a certain level before the IEFCC flat top was reached. The density pumpout depends on both the plasma responses to the $n = 2$ fields and the change of ELM frequency, but not the amplitude of IEFCC. However, saturation of the plasma density pump-out was rather slow and it was delayed by $\sim 300\text{ms}$ after the change of ELM frequency saturated. This time delay might be due to differences in the time scales of the MHD response and the plasma confinement.

The saturation effect of the plasma response has also been studied for plasmas with different plasma currents from 1.2 to 1.6 MA. In this experiment, the toroidal fields for those discharges are the same (1.85T). The threshold of the plasma response saturation depends on the plasma current, and it is lower for plasmas with low current as shown in Fig.5. It should be noted that the change of plasma current with a constant B_t will also change the edge safety factor as well. The q_{95} for these

three discharges is 3.0 (82470), 3:5 (82469) and 4.0 (82471), respectively. Significant non-resonance magnetic plasma rotation braking has been observed. The change of plasma rotation depends on the amplitude of I_{EFCC} , and it was not saturated even with the maximal value of IEFCC.

2.2 MULTIPLE SPLITTING OF THE OUTER STRIKE POINT DURING THE ELM CRASH

Multiple splitting of the strike point, appearing in the ELM heat flux profiles measured by a fast IR camera [16,17] along the outer divertor plate, has been observed for the first time during the application of the $n=2$ fields on JET.

Figure 6 shows the I_{EFCC} dependence of the heat flux profiles measured along the outer divertor plates for one of the pulses shown in Fig.1. Without the $n=2$ fields, the maximal ELM peak heat flux is normally located at the original strike point (OSP). The natural ELM filaments [18] [19] can carry a small amount of heat fluxes, propagate out of the plasma and deposit the heat on either the wall or the divertor plates. They appear as multiple small peaks on the heat flux profiles on the divertor plate, but their locations are highly random and shifting in time. When the $n=2$ field was applied, the multiple splitting of the OSP was seen during the ELM crash, and the maximal ELM peak heat flux was reduced due to redistribution of the heat fluxes from the OSP to the secondary strike points (SSPs). Some of the SSPs near the OSP can even carry the same amount of heat fluxes as that by the OSP. Those SSPs do not move and disappear in a short time (~ 1 ms) after the ELM crash. The locations of those SSPs depend on the amplitude of IEFCC as well as the edge safety factor. Those observations are consistent with modelling of the manifold structure formation at the plasma edge, especially near the X point of the separatrix, with a 2D plasma equilibrium perturbed by a 3D RMP field [20]. The 3D feature of the divertor footprints can be induced by the interaction of the manifold structures with the divertor plates. The field lines inside the manifold structures are originally from the plasma region with good confinement. Once those field lines connect to the divertor plates, more high-energy particles can be carried out from the hot plasma region along the field lines toward the divertor. This can be a possible mechanism of both reduction of the maximal ELM peak heat fluxes on the OSP and a large amount of heat fluxes deposited at the SSPs.

Statistical analysis shows a reduction from ~ 22 to ~ 8 MW/m² of the maximal peak heat fluxes due to ELMs when the frequency of the Type-I ELMs increased from ~ 20 to ~ 80 Hz with the $n=2$ fields as shown in Fig.7. Due to a toroidal dependence of the divertor footprints with 3D magnetic perturbations, to date, it is difficult to calculate the ELM wetted area based on one local divertor heat flux measurement. However, it is very clear that multiple splitting of the OSP induced by RMP fields helps a further reduction of the maximal ELM peak heat fluxes beside mitigation of the ELM size.

3. ELM CONTROL IN HIGH COLLISIONALITY H-MODE PLASMAS WITH THE ILW

Strong mitigation of type-I ELMs has been observed with the application of an $n=2$ field in high

collisionality H-mode plasmas on the JET tokamak with the ILW. In this experiment, the target plasma had a low triangularity shape ($\delta_{\text{average}} = 0.26$) with a toroidal magnetic field of $B_t = 1.85\text{T}$ and a plasma current of $I_p = 1.2\text{MA}$, corresponding to an edge safety factor of $q_{95} = 4.8$. The type-I ELMy H-mode was sustained for 5 seconds by NBI with an input power of 2.6MW. Strong gas puffing with a constant rate of 4×10^{21} e/s was applied during the NBI heated phase. During the H-mode phase, the Greenwald fraction of plasma density is ~ 0.8 and the electron collisionality at the pedestal, ν_e^* , is ~ 2.0 .

Figure 8 shows an example of type-I ELM mitigation with $n = 2$ fields from this experiment. The $n = 2$ perturbation field created by the EFCCs has a slow ramp-up for 2s, and a flat top for 1s which is a factor of ~ 4 longer than the plasma energy confinement time. As soon as I_{EFCC} reached a critical value of 44kAt, the ELM frequency started to increase. With further increase of I_{EFCC} , the type-I ELMs with frequency of $\sim 45\text{Hz}$ were replaced by high frequency (a few hundred Hz) small ELMs. The drop in the pedestal temperature due to the mitigated ELMs, $T_e^{\text{ped}} = T_e^{\text{ped}}$, was less than 3%, while it is $\sim 16\%$ for the unmitigated ELMs as seen in Fig.9 a) and b). There is no drop in the core electron density and temperature during the application of the $n = 2$ field even with I_{EFCC} up to 88kAt. The influence of the $n = 2$ field on the edge pedestal can also be neglected as seen in Fig.10. Although the pedestal density and temperature vary slightly due to non-stationary features of the discharge, the pedestal pressure remains the same within the measurement error. The H-factor (H98y) in this high collisionality target plasma is only 0.65, and it is weakly influenced by the application of $n = 2$ fields. During the normal type-I ELMy H-mode phase, the maximal surface temperature (T_{max}) on the outer divertor plate was increased overall and associated with large periodical variations due to the type-I ELMs as seen in Fig.11. However, during the application of the $n = 2$ field, T_{max} was saturated and has only small variations of a few degrees due to the small mitigated ELMs. Splitting of the outer strike point has been observed for the first time during the strong mitigation of the type-I ELMs with an $n = 2$ field on JET as seen in Fig.11 (top).

Figure 12 shows extended time traces of the EFCC coil current, intensity of D_α emission, $n = 1$ and $n = 2$ plasma responses during the slow ramp-up of the EFCC current. Saturation of the $n = 2$ plasma response occurs much earlier even with a small amplitude of I_{EFCC} , and is not correlated with the change of ELM behaviour. However, the $n = 1$ plasma response appears at the time when the ELM frequency increases. This is different to observations in low collisionality plasmas, where only the $n = 2$ plasma response was observed, and the $n = 1$ plasma response can be neglected. Significant plasma rotation braking has also been observed when an $n = 2$ field was applied. The Sawtooth Precursor mode frequency was reduced from 4.5kHz down to a value closer to zero when the I_{EFCC} was ramped up to 88 kAt.

4. DISCUSSION

On JET, to date, no complete ELM suppression has been observed by application of either $n = 1$ or $n = 2$ fields with a Chirikov parameter well above one $\sqrt{\Psi} \geq 0.925$, which is one of the important

criteria for the design of ITER ELM control coils. Regarding on the applied perturbation fields, the major difference in the ELM control/suppression experiments from JET and DIII-D is the magnetic perturbation spectra (not only the mode number, but also the ratio of the resonant to the non-resonant components). However, on DIII-D, large type I ELMs were also suppressed by $n = 3$ fields induced by a single row of off-midplane in-vessel coils in H-mode plasmas at the low pedestal collisionality ($\nu_e^* \sim 0.1$) [21]. The perturbation spectrum induced by a single row of coils is different to that with both up-down coils. In addition, recent results from AUG also demonstrate that ELM mitigation can be achieved by application of $n = 2$ non-axisymmetric magnetic perturbations with either resonant or nonresonant configurations in high density ELM H-mode plasmas [7]. Therefore, the present JET results indicate that there is an additional mechanism for ELM mitigation/suppression with perturbation fields.

The preliminary results from JET with the ILW show a significant effect of the wall condition on the ELM control with $n = 2$ fields. With the CFC-wall, the previous experimental results show no clear effect of low n ($n = 1$ or 2) fields on the high collisionality ($\nu_e^* \geq 2.0$) ELM H-mode plasmas except braking of the plasma rotation [23]. However, with the ILW, strong mitigation of type-I ELMs is observed when an $n = 2$ field is applied in high collisionality ($\nu_e^* \sim 2:0$) H-mode plasmas. Splitting of the outer strike point is seen but no density pump-out effect is observed during the mitigation of the type-I ELMs with $n = 2$ fields. These experimental observations are similar to those in high density ELM mitigation experiments with an $n = 2$ field on AUG, which is equipped with a full Tungsten wall [7].

For the first time the saturation effect of plasma response to the applied $n = 2$ magnetic perturbations has been observed in low collisionality H-mode plasmas on JET with the ILW. A strong increase in ELM frequency and a drop in density are observed when the transition from linear to non-linear plasma responses occurs. Here, the linear response might correspond to the ideal MHD plasma response to the applied $n = 2$ fields, while the non-linear response might be the resistive MHD plasma response with formation of edge magnetic islands (so called field penetrations) [24] [25]. This can explain the strike point splitting observed on the outer divertor plates during ELM crashes.

The saturation effect of plasma response has not been observed before on JET with CFC-wall, where the ELM frequency increases with further increasing of I_{EFCC} after an ELM mitigation threshold of $IEFCC$ is reached [22]. The results indicate the limitation of ELM mitigation may not be due to amplitude of applied perturbations or the maximal coil currents, but can be due to the target plasma itself. Therefore, it is urgent and important to prove the applicability of the ELM control / suppression with perturbation fields in the plasma with ITER-like PFCs. Investigation of the plasma reaction to the perturbation field could be the key to understand the physical mechanism of ELM control/ suppression with perturbation fields.

CONCLUSION

ELM mitigation with $n = 2$ magnetic perturbations induced by the EFCCs has been performed with

the ILW. The preliminary results show that strong mitigation of type-I ELMs is observed when an $n = 2$ field is applied in high collisionality ($\nu_e^* = 2.0$) Hmode plasmas. No density pump-out effect has been observed. Splitting of the outer strike point has been observed during the mitigation of the type-I ELMs. In the low collisionality type-I ELMy H-mode plasmas with the ITER-like wall, a saturation effect of ELM mitigation and a reduction of the maximal ELM peak heat load due to the multiple splitting of the outer strike point have been observed during the application of $n = 2$ fields. Those were not observed in the previous EFCC ELM control experiments with the CFC-wall on JET. The preliminary results indicate that there are two possible ways of mitigating the ELM heat loads: i) increase ELM frequency and reduce the ELM energy losses, or ii) widen the wetted area of the ELM heat fluxes on the divertor plates.

ACKNOWLEDGEMENTS

This work was supported by EURATOM and carried out within the framework of the European Fusion Development Agreement. The views and opinions expressed herein do not necessarily reflect those of the European Commission. Supported from the Helmholtz Association in frame of the Helmholtz-University Young Investigators Group VH-NG-410 is gratefully acknowledged.

REFERENCES

- [1]. ITER Physics Basis, Nuclear Fusion, **39**, 2137 (1999).
- [2]. F. Wagner, et al., Physical Review Letters **49**, 1408 (1982).
- [3]. T. E. Evans, et al., Nature of Physics **2**, 419 (2006).
- [4]. Y. Liang, et al., Physical Review Letters **98** 265004 (2007).
- [5]. A. Kirk, et al., Nuclear Fusion, **50**, 034008 (2010).
- [6]. J. M. Canik et al., Nuclear Fusion, **50**, 034012 (2010).
- [7]. W. Suttrop, et al., Physical Review Letters **106**, 225004 (2011).
- [8]. Y. M. Jeon, et al., Physical Review Letters **109** 035004 (2012)
- [9]. Y. Liang, et al., Plasma Phys. Control. Fusion **49** B581 (2007).
- [10]. Y. Liang, et al., Nuclear Fusion **50** 025013 (2010).
- [11]. Y. Liang, et al., Physical Review Letters **105** 065001 (2010).
- [12]. Y. Liang, et al., Nuclear Fusion **51** 073001 (2011).
- [13]. V. Philipps, et al., Fusion Engineering and Design **85**, 1581 (2010).
- [14]. R. Pasqualotto, et al., Review of Scientific Instruments **75**, 3891 (2004).
- [15]. M. N. A. Beurskens, et al., Plasma Physics and Controlled Fusion **51**, 124051 (2009).
- [16]. T. Eich, et al., Journal of Nuclear Materials **415**, S856 (2011).
- [17]. I. Balboa et al., Review of Scientific Instruments **83**, 10D530 (2012)
- [18]. T. Eich, et al., Physical Review Letters **91** 195003 (2003)
- [19]. S. Devaux, et al., Journal of Nuclear Materials, **415** S865 (2011)
- [20]. M. Rack, et al., Nuclear Fusion **52** 074012 (2012).

- [21]. Fenstermacher M.E. et al. Nuclear Fusion **48** 122001 (2008)
- [22]. Y. Liang, et al., Journal of Nuclear Materials, **390-91** 733, (2009).
- [23]. Y. Sun et al., Plasma Physics and Controlled Fusion, **52** 105007 (2010).
- [24]. Y. Yang, et al., Nuclear Fusion **52** 074014 (2012).
- [25]. M. Becoulet, et al., Nuclear Fusion **48**, 024003 (2008).

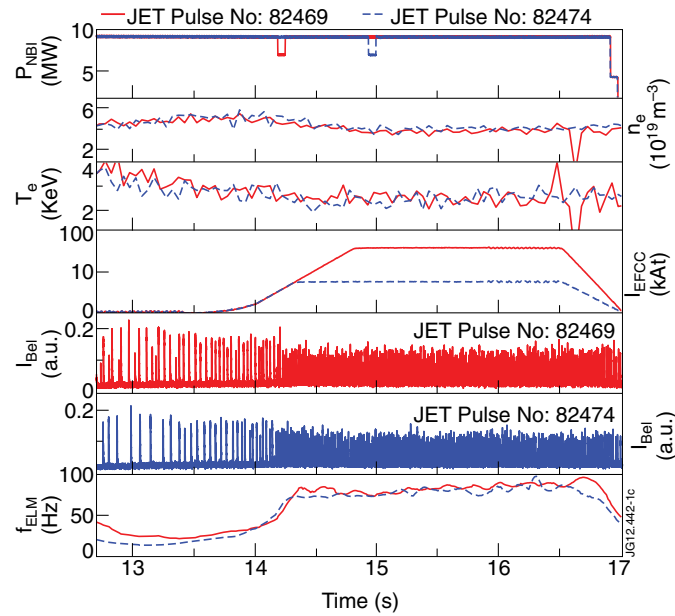


Figure 1: Comparison of ELM mitigation with an $n = 2$ field in low collisionality H-mode plasmas between two discharges with EFCC coil currents of 2.5 (dashed) and 5.5kA (solid), respectively. The signals from top are total NBI input power, plasma core density, electron temperature, EFCC coil currents, intensity of Be-I emission, and ELM frequency.

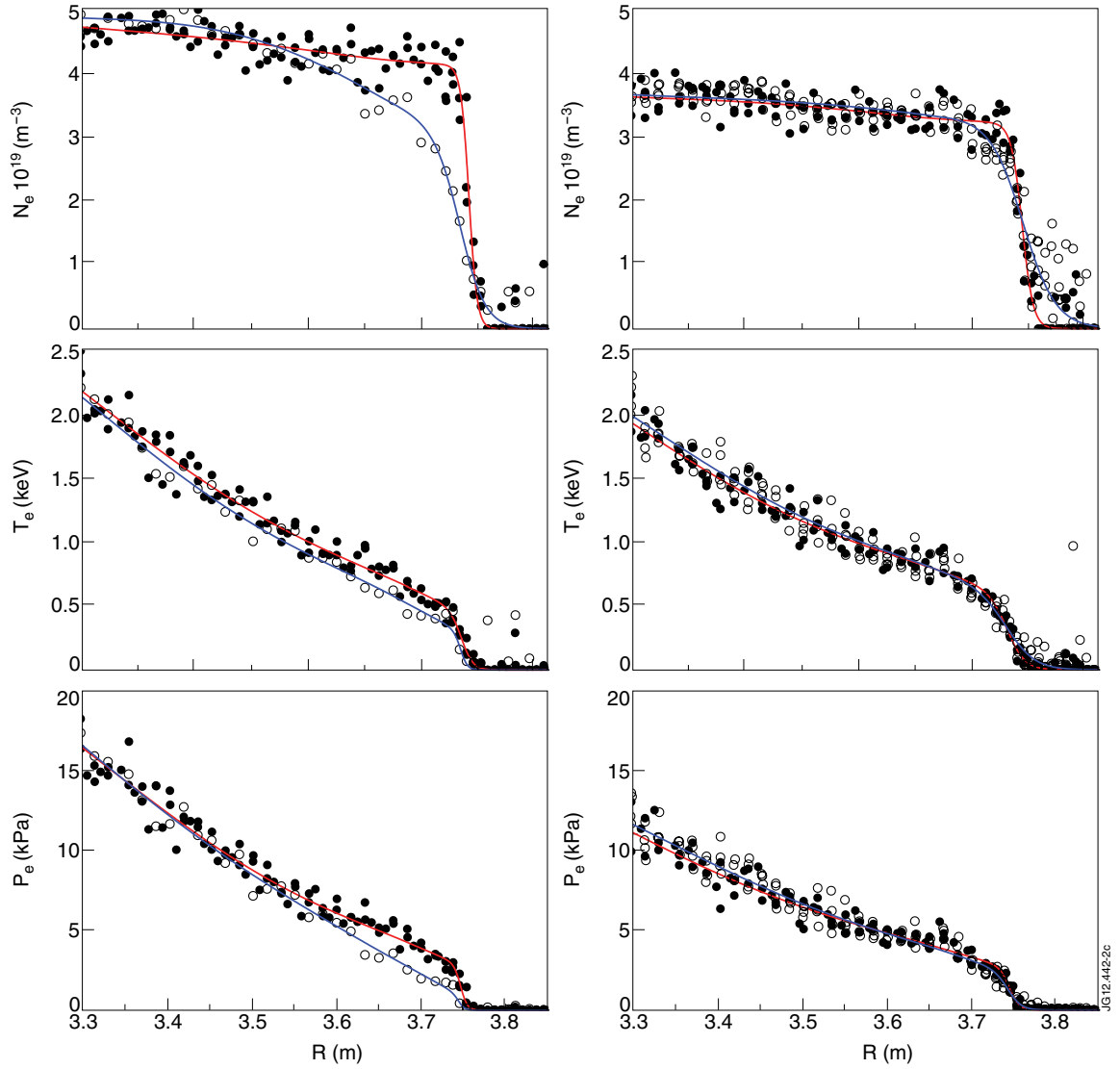


Figure 2: Pedestal profiles measured before (closed circles) and after (open circles) an ELM for the (left) unmitigated type-I ELMs and (right) mitigated small ELMs with $n = 2$ fields for the Pulse No: 82474 seen in Figure 1. The profiles are averaged over several ELMs, and measured during 1–20% ELM circle for the case after ELM crash and 70–99% for the case before ELM crash.

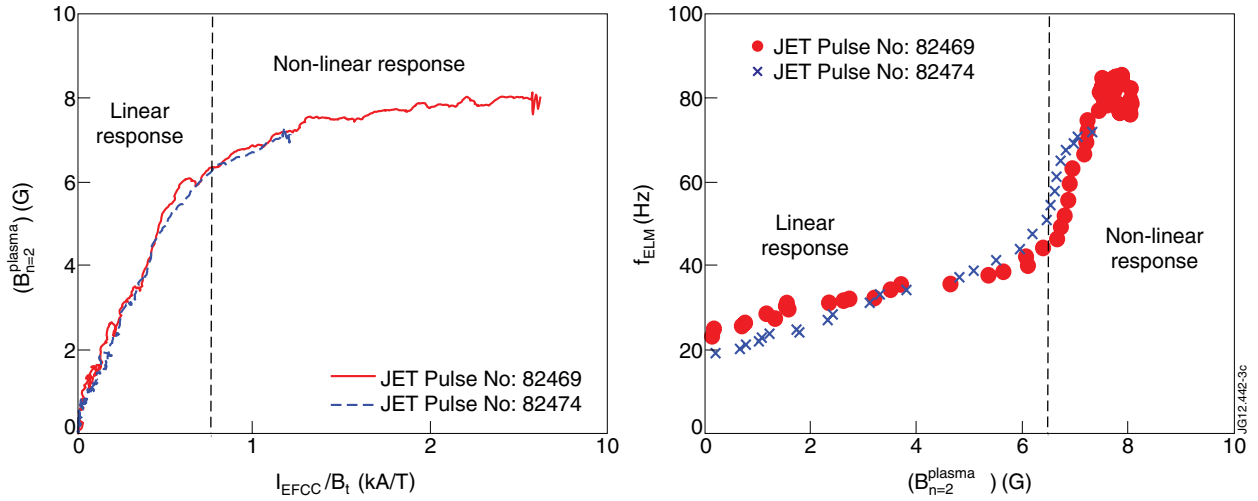


Figure 3: (left) Plasma responses to the applied $n = 2$ fields, $|B_{n=2}^{plasma}|$, as a function of I_{EFCC} normalized to the toroidal field; (right) ELM frequency as a function of $|B_{n=2}^{plasma}|$ for the two pulses shown in Figure 1. The dashed vertical line indicates the threshold of transition from linear to non-linear plasma responses.

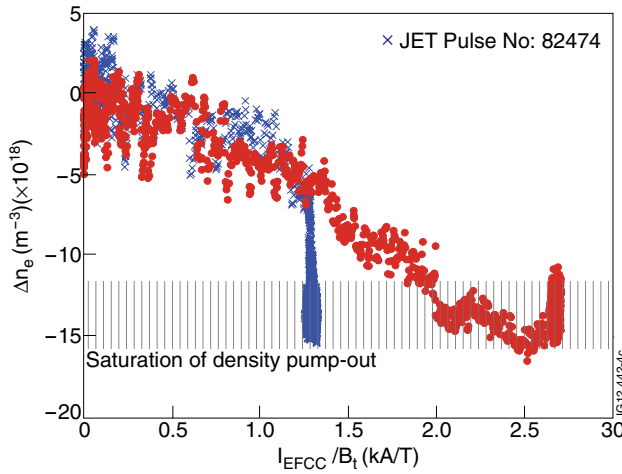


Figure 4: Change of the central line averaged density as a function of the normalized $n = 2$ perturbations for the two discharges shown in figure 1.

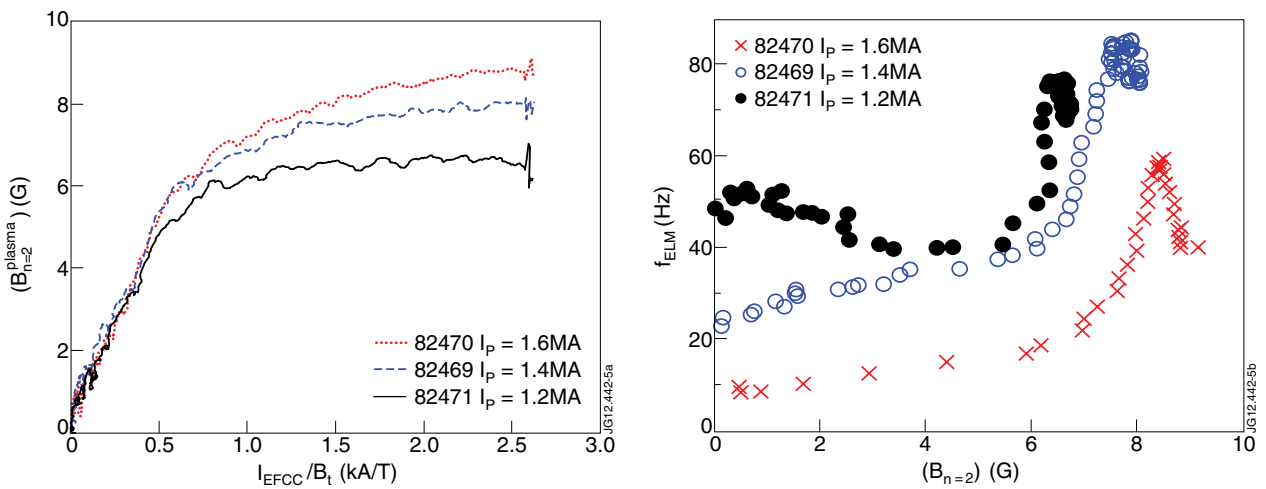


Figure 5. (top) Plasma responses, $|B_{n=2}^{plasma}|$, to the applied $n = 2$ fields as a function of I_{EFCC} normalized to the toroidal field; (bottom) ELM frequency as a function of $|B_{n=2}^{plasma}|$ for three pulses with different plasma currents.

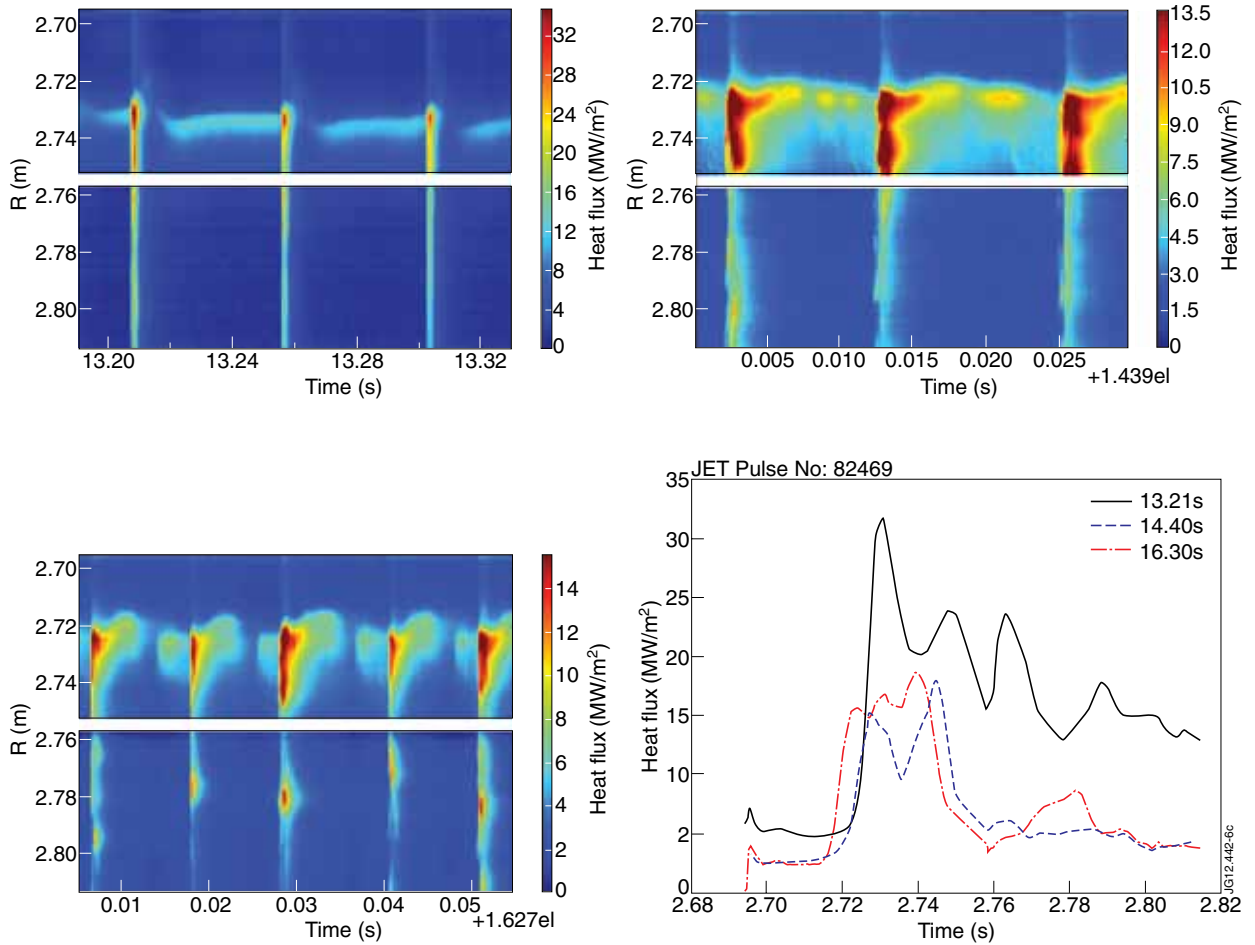


Figure 6: Extended time traces of the heat flux distribution on the outer divertor plate in the phases (upper left) without $n = 2$ field, (upper right) with $I_{EFCC} = 44kAt$ and (lower left) with $I_{EFCC} = 88kAt$. (lower right) ELM peak heat flux profiles along the outer divertor measured from those three different phases.

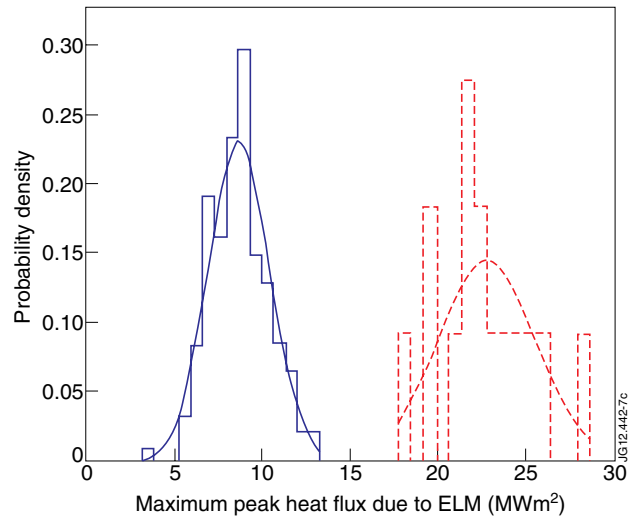


Figure 7: Statistical analysis of the maximal peak heat fluxes due to the unmitigated ELMs (dashed) and the mitigated (solid) ELMs with $n = 2$ fields for the Pulse No: 82469 shown in Figure 1.

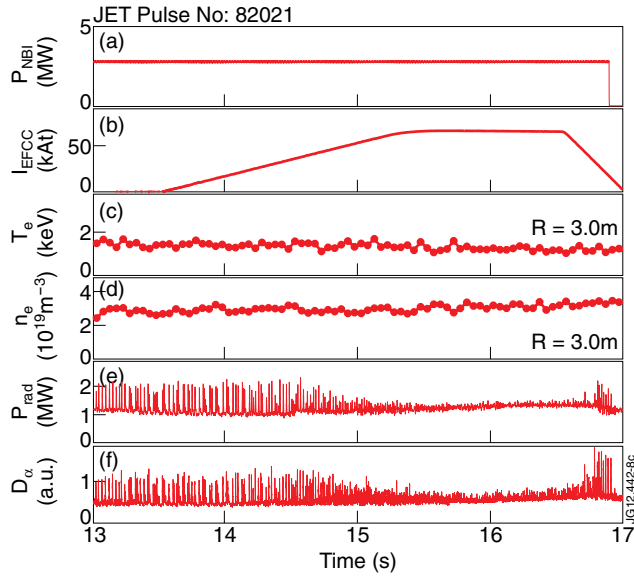


Figure 8: Overview of a type-I ELM mitigation experiment on JET. The traces from top to bottom are the NBI input power (P_{NBI}), the EFCC coil current (I_{EFCC}), the central plasma electron temperature (T_e) and density (n_e) measured at $R = 3.0\text{m}$, the total plasma radiation power (P_{rad}), and the D_α emission signals measured at the inner divertor.

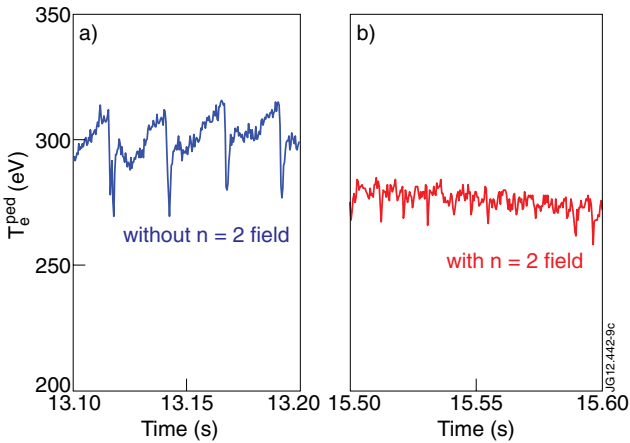


Figure 9: Time evolution of the pedestal electron temperature measured a) without and b) with $n = 2$ fields. Here, the electron temperature is measured by the electron cyclotron emission (ECE) measurement.

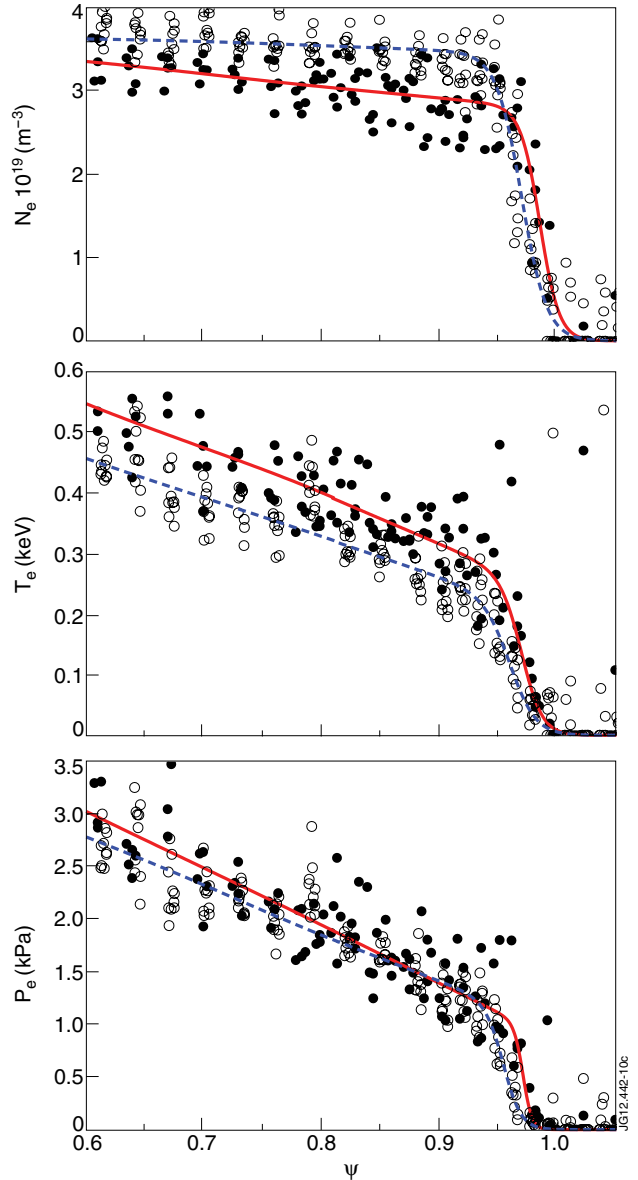


Figure 10: Radial profiles of the (top) pedestal density, (middle) electron temperature and (bottom) pressure measured with (open circles) and without (closed circles) the $n = 2$ fields. The profiles are selected in the 40–99% of the ELM cycle and averaged several ELMs over 0.5 seconds for the pre-EFCC and 1.5 seconds for the EFCC phases.

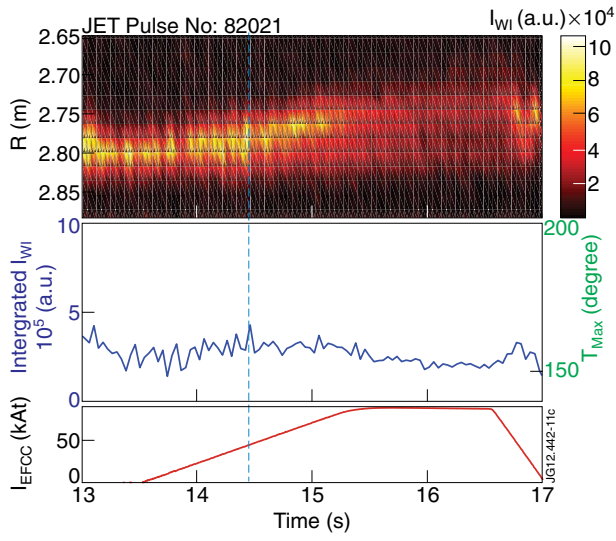


Figure 11: Time evolutions of (top) intensity profile of W-I emission (I_{W-I}), (middle, blue) integrated W-I emission, and (middle, green) maximal surface temperature on the outer divertor plate, and (bottom) the EFCC coil current.

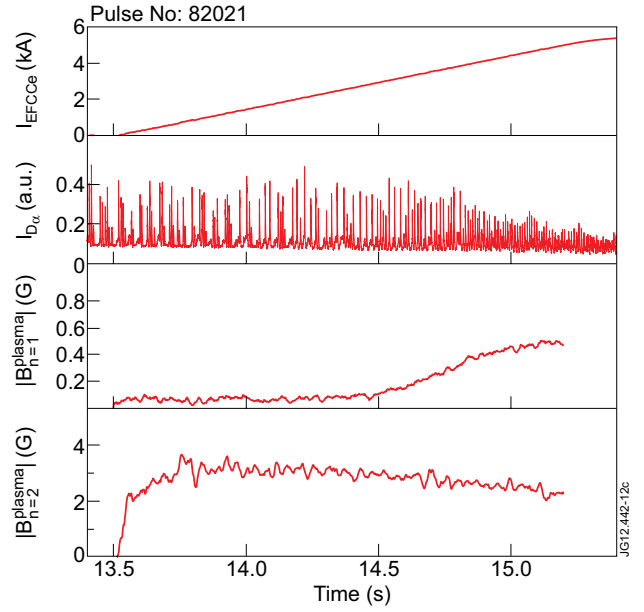


Figure 12: Extended time trace of (a) EFCC coil current (I_{EFCC}), (b) Intensity of D_α emission, (c) $n = 1$ radial field and (d) Plasma responses to the applied $n = 2$ fields.